Check for updates

Biosensors

Deutsche Ausgabe: DOI: 10.1002/ange.201910772
Internationale Ausgabe: DOI: 10.1002/anie.201910772

Exploring the Trans-Cleavage Activity of CRISPR-Cas12a (cpf1) for the Development of a Universal Electrochemical Biosensor

Yifan Dai, Rodrigo A Somoza, Liu Wang, Jean F. Welter, Yan Li, Arnold I Caplan* und Chung Chiun Liu**

Abstract: *An accurate, rapid, and cost-effective biosensor for the quantification of disease biomarkers is vital for the development of early-diagnostic point-of-care systems. The recent discovery of the trans-cleavage property of CRISPR type V effectors makes CRISPR a potential high-accuracy bio-recognition tool. Herein, a CRISPR-Cas12a (cpf1) based electrochemical biosensor (E-CRISPR) is reported, which is more cost-effective and portable than optical-transduction-based biosensors. Through optimizing the in vitro trans-cleavage activity of Cas12a, E-CRIPSR was used to detect viral nucleic acids, including human papillomavirus 16 (HPV-16) and parvovirus B19 (PB-19), with a picomolar sensitivity. An aptamer-based E-CRISPR cascade was further designed for the detection of transforming growth factor β1 (TGF-β1) protein in clinical samples. As demonstrated, E-CRISPR could enable the development of portable, accurate, and cost-effective point-of-care diagnostic systems.*

Introduction

An accurate, rapid, and cost-effective sensing strategy for the quantification of disease biomarkers is vital for the development of early-diagnostic point-of-care systems, further leading to personalized medicine and benefiting overall human health. Electrochemistry-based biosensing platforms have been widely developed, owing to its rapid signal readout, affordable transduction element, and simple sensing platform.[1] One of the critical challenges for such a sensing system is its accuracy. Recent robust developments of CRISPR (clustered regularly interspaced short palindromic repeats) based gene editing systems demonstrated the accuracy of the CRISPR system in targeting nucleic acids, owing to the complementarity-dependent CRISPR cleavage event.[2] Utilizing collateral cleavage of the nonspecific ssDNA reporter (termed trans-acting cleavage), initiated by the recognition and cleavage of the target DNA (termed cis-acting cleavage) by Cas-crRNA, CRISPR type III, V, and VI RNA-guided nucleases (Csm6, Cas12a, Cas13) have been used for the detection of nucleic acids (RNA/DNA) through fluorescent transduction systems.[3] Herein, we extend the application of the CRISPR-Cas12a (cpf1) system to the development of an electrochemical biosensing system because of its relative cost-efficiency and the portable nature of the transduction system compared with the fluorescent transducer. Moreover, for a comprehensive and robust point-of-care system, a potential universal biosensing platform that can detect different categories of analytes is of high importance for clinical applications. Therefore, building upon the accurate CRISPR-based sensing system, we further design a Cas12a-based biosensing cascade as a strategy for protein detection. Our study demonstrates a CRISPR-Cas12a (cpf1) based electrochemical biosensing platform (E-CRISPR) for the detection of the major categories of biomolecules, providing a potential deployable point-of-care system for the healthcare industry.

E-CRISPR is a simple endonuclease activity transduction method for CRISPR type III, V, VI nuclease-based sensing systems and enables the detection of multiple analyte classes. A disposable, micro-fabricated gold-based three-electrode sensor with gold as working and counter electrodes and Ag/AgCl as the reference electrode was applied for the development of the electrochemical biosensor (Supporting Information, Figure S1).[4] The Cas12a-crRNA duplex is designed to specifically recognize and cleave a target nucleic acid strand based on the protospacer adjacent motif (PAM) sequence of the target and complementarity between the target and the crRNA (Figure 1 A).[5] PAM recognition depends on the specific 5′-TTTN nucleic acid sequence located in the opposite strand (blue strand) to the recognition strand (orange strand). Only upon the recognition of the PAM sequence by the Cas protein, the Cas protein, acting as a DNA helicase, unwinds the target DNA. After the separation of the target strands, the complementarity (between crRNA and target) dependent cleavage activity can further be activated.[6] To achieve the electrochemical transduction of the CRISPR detection signal, the cis-cleavage-initiated trans-cleavage effect of Cas12a on the nonspecific ssDNA is probed through an electrochemical method. A nonspecific ssDNA reporter is designed with a methylene blue (MB) electrochemical tag for

[*] Y. Dai, Prof. C. C. Liu
Department of Chemical and Biomolecular Engineering, Electronics Design Center, Case Western Reserve University Cleveland, OH 44106 (USA)
E-Mail: yxd176@case.edu
cxl9@case.edu
Dr. R. Somoza, Prof. J. F. Welter, Prof. A. I Caplan
Department of Biology, Skeletal Research Center & Center for Multimodal Evaluation of Engineered Cartilage, Case Western Reserve University, Cleveland, OH 44106 (USA)
E-Mail: aic@case.edu
Dr. L. Wang, Prof. Y. Li
Department of Genetics and Genome Sciences, School of Medicine, Case Western Reserve University, Cleveland, OH 44106 (USA)
Supporting information and the ORCID identification number(s) for the author(s) of this article can be found under: https://doi.org/10.1002/anie.201910772.

 © 2019 Wiley-VCH Verlag GmbH & Co. KGaA, Weinheim

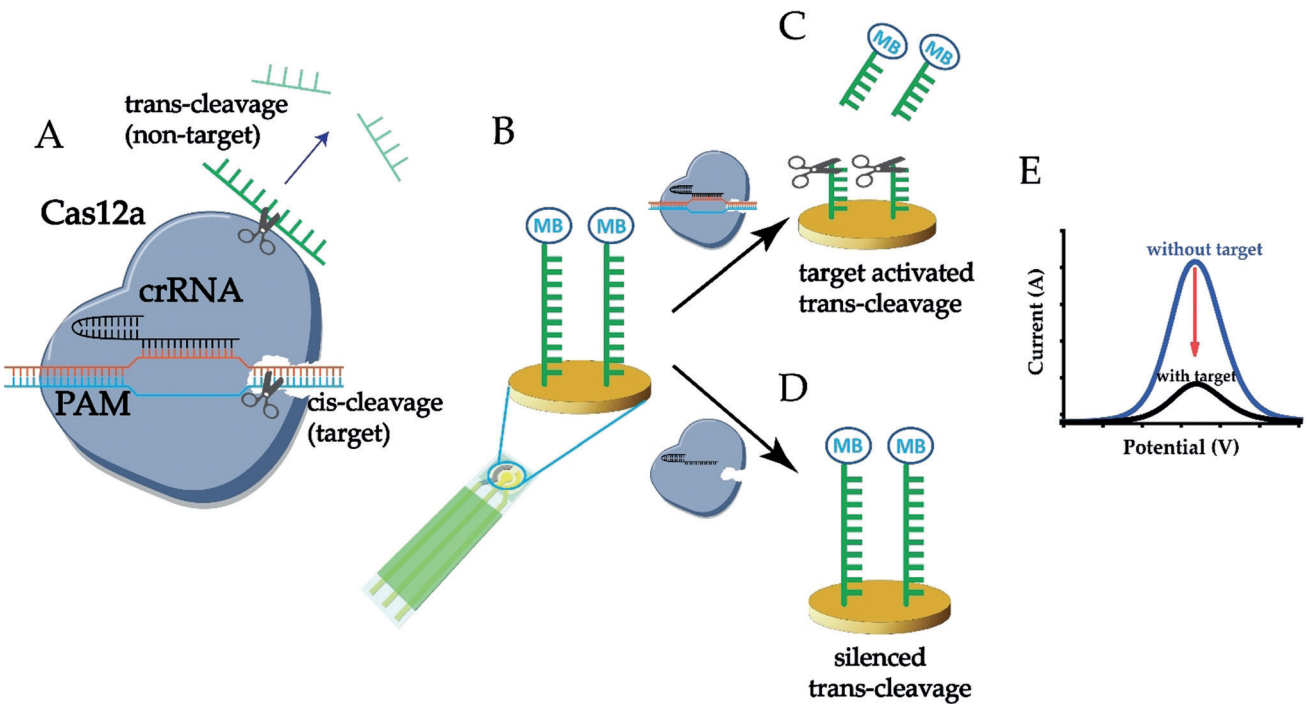


Figure 1. Principle of E-CRISPR. A) Cas12a (cpf1) performs crRNA-guided trans-cleavage of nonspecific ssDNA, initiated by the cis-cleavage of specific DNA. B) Nonspecific ssDNA reporter with methylene blue tag immobilized on the gold electrode. C) In the presence of the target, Cas12a-crRNA would initiate the trans-cleavage of the nonspecific ssDNA reporter, resulting in a low electrochemical current of methylene blue. D) In the absence of the target, Cas12a-crRNA would not initiate the trans-cleavage of the nonspecific ssDNA reporter, resulting a high electrochemical current of methylene blue. E) A representation of electrochemical current outputs in the absence and presence of the target.

signal transduction and a thiol moiety to tether on the sensor surface in order to acquire the signal electrically (Figure 1B).[7] Consequently, the electron transfer process between the gold electrode and the redox active species on the ssDNA can be electrochemically initiated and transduced. With the presence of the target, the Cas12a trans-cleavage activity is activated, cleaving the MB-ssDNA reporter off the electrode surface, therefore decreasing the MB signal transduced (Figure 1C). In the absence of the target, the Cas12a trans-cleavage activity is silenced, retaining the MB-ssDNA reporter on the surface (Figure 1D). A representation of electrochemical signal output based on the conditions without/with target is shown in Figure 1E. The design of the MB-ssDNA-coated electrode is generally applicable for any CRISPR type III, V, and VI systems as a simple and cost-effective CRISPR activity transduction strategy. Based on the concept of E-CRISPR, we developed this platform as a universal biosensing strategy for the detection of nucleic acid and protein.

Results and Discussion

Verification of E-CRISPR for Nucleic Acid Detection

To examine the feasibility of the E-CRISPR for nucleic acid detection, a human papilloma virus (HPV) subtype, HPV-16, which is critical to carcinogenesis,[8] was selected as the target. A target sequence in the L1-encoding gene of HPV16 was identified based on the TTTN PAM sequence required by the Cas12a endonuclease.[9] The electrochemical biosensing platform was initially developed based on the Cas12a endonuclease from *Acidaminococcus sp.* (AsCas12a).[10] We first investigated the on-chip collateral cleavage performance based on the AsCas12a-crRNA duplex targeting the HPV-16 sequence. After assembling the HPV-16 and the AsCas12a-crRNA, the triplex complex was directly incubated on the ssDNA -reporter-coated electrode. Square wave voltammetry (SWV) was applied to evaluate the MB signal, which was decreased only in the presence of the cognate target with the corresponding AsCas12a-crRNA (Figure 2A).

Evaluation of the Optimized Condition for On-Chip Trans-Cleavage Activity

For biosensing, the detection sensitivity is critical due to the low abundance of clinically relevant biomarkers in human fluids.[11] For the E-CRISPR detection platform, the trans-cleavage activity is the key for signal transduction, and therefore is critical to the sensitivity performance. We first compared the on-chip trans-cleavage activity of another type of Cas12a protein, *Lachnospiraceae* bacterium ND2006 Cas12a (LbCas12a),[12] with AsCas12a. LbCas12a demonstrated a more apparent and stable trans-cleavage response within 5 min compared with that of AsCas12a (Figure 2B). LbCas12a presented a more robust trans-cleavage activity within the testing period using the same experimental

 © 2019 Wiley-VCH Verlag GmbH & Co. KGaA, Weinheim

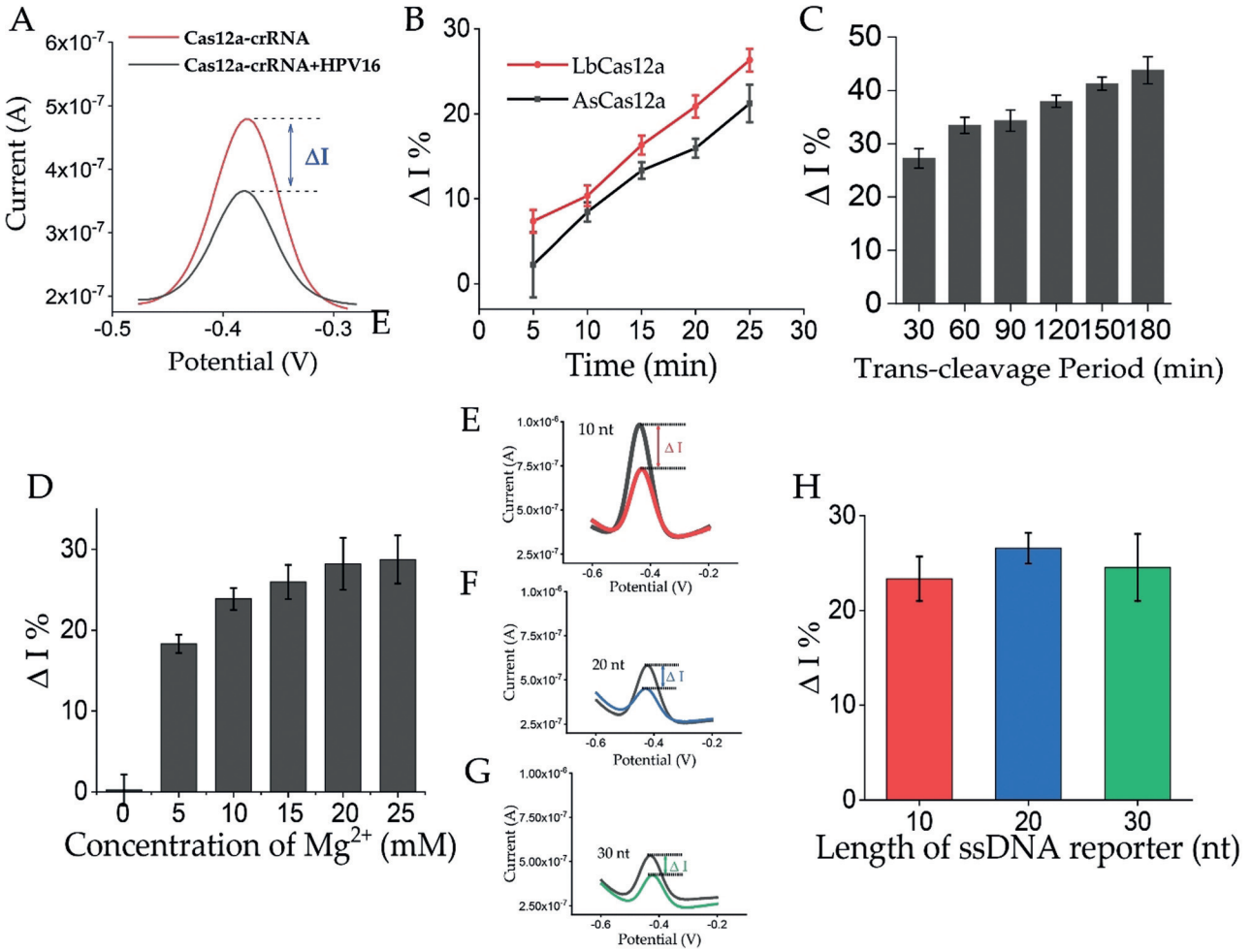


Figure 2. Optimization of on-chip trans-cleavage activity. A) Representation of square wave voltammetry (SWV) evaluation of E-CRISPR in response to HPV-16. Red curve represents the background signal of 50 nM of Cas12a-crRNA duplex. Black curve represents the signal generated by the target-induced trans-cleavage activity of 50 nM of Cas12a-crRNA. B) Evaluation of 50 nM of Cas12a orthologues from *Lachnospiraceae* and *Acidaminococcus sp.* on its activity for on-chip trans-cleavage activity based on the change of current between background signal and target-mediated signal. $\Delta I\% = \frac{\text{Background signal} - \text{Target signal}}{\text{Background signal}}$ (red line: LbCas12a; black line: AsCas12a). C) Evaluation of trans-cleavage activity using 50 nM of LbCas12a-crRNA-target triplex. D) Evaluation of the effect of the concentration of divalent metal ions on the trans-cleavage activity of the RuvC domain using 50 nM of LbCas12a-crRNA-target triplex. E,F,G) SWV graphs of different lengths of surface ssDNA reporters based on 30 nM of LbCas12a-crRNA-target triplex. H) Comparison of signal change from different lengths of surface ssDNA reporters. SWV graphs in these figures present the result of a single test. Error bars in figures present the standard error (SE) based on at least three individual tests using at least three different sensors.

conditions, therefore LbCas12a was selected for further E-CRISPR development. We further evaluated the possible factors that may affect the trans-cleavage activity for on-chip electrochemical test using HPV-16 as the target. The optimal trans-cleavage period was investigated. The $\Delta I\%$ continuously increased with increasing incubation time for the collateral cleavage event (Figure 2C). It is interesting to notice that trans-cleavage does not occur simultaneously with cis-cleavage. The cis-cleavage of target strand is typically finished within 30 min;[3a] however, the trans-cleavage function remained active even after 3 hours (Figure 2C), indicating that the target recognition initiated cis-cleavage activity of the Cas12a system is the activator for the trans-cleavage functional domain of the Cas12a endonuclease.

We further investigated the chemical environment of the Cas12a to optimize the trans-cleavage performance. An important factor that may affect the Cas12a cleavage activity is the divalent cation Mg^{2+} concentration in the testing solution.[13] Cas12a RuvC domain is known to cleave ssDNA through the two-metal ion mechanism,[14] in which the Mg^{2+} ions induce conformational coordination of the RuvC domain and the ssDNA by shifting the spatial distribution of ssDNA around the RuvC active cutting center. Therefore, we evaluated the effect of concentration of Mg^{2+} ions in the in vitro cleavage solution on the activity of trans-cleavage function. The trans-cleavage activity was only activated with the presence of the Mg^{2+} ions in the testing solution (Figure 2D). Increasing concentration of Mg^{2+} cations up to 15 mM demonstrated an enhanced trans-cleavage activity. Hence, an optimized Mg^{2+} concentration of 15 mM was selected for the preparation of the Cas12a-crRNA duplex.

© 2019 Wiley-VCH Verlag GmbH & Co. KGaA, Weinheim

In order to perform an efficient surface-chemistry-based trans-cleavage, the accessibility of Cas12a endonuclease to the nonspecific ssDNA is important. Thus, we evaluated the effect of ssDNA reporter density on the electrode surface on the variation of electrochemical signal before and after the trans-cleavage activity. An ideal surface condition can provide an optimized electrostatic environment for charged phosphate backbones and the hydroxyl groups of the passivation agents to ensure an upright ssDNA surface, facilitating the cleavage activity. The surface density of ssDNA reporter was manipulated by the concentration of the ssDNA reporter incubation solution. As shown in Figure S2 A in the Supporting Information, a high surface density of ssDNA reporter significantly decreased the change of signal, because this high surface density decreased the accessibility of Cas endonuclease to the ssDNA reporter, producing a steric hindrance effect, which limited the trans-cleavage activity. An ideal density was prepared using 1 μM of ssDNA reporter and identified as 5.2×10^{-14} mol mm^{-2} (Supporting Information, Figure S2 B), which created sufficient space for Cas12a to perform collateral cleavage on the electrode surface, providing a sufficient electrochemical signal change and ensuring an excellent detection resolution.

Other than the surface density, the length of the immobilized ssDNA reporter was also evaluated. We hypothesized that ssDNA reporters with different lengths might lead to different cleavage efficiency due to the exposed length difference. Different lengths of ssDNA probes at the same concentration were evaluated using the same reaction conditions of E-CRISPR as investigated previously. Moreover, the effect of passivation agents with different carbon chain lengths may influence the electrostatic interaction between the phosphate backbones of ssDNA probes, therefore this was also evaluated for optimal cleavage activity (Supporting Information, Figure S3). The selected ssDNA and passivation agent pairs were then compared through the effect of lengths on trans-cleavage activity. However, different lengths of ssDNA reporter only produce a minute variation (less than 5%) in signal change (Figure 2 H). We observed that for a short ssDNA reporter (10 nt), the electrochemical oxidation current over the background current was larger than that of a long ssDNA strand because of its short contact-mediated electron tunneling distance to the electrode, resulting faster charge transfer kinetics (Figure 2 E). Therefore, the short probe possessed a large baseline current. As for long reporters (20 nt and 30 nt), they gave a relative low background current (Figure 2 F,G), but the ΔI% of these long reporters were comparable to that of short reporter. 20 nt ssDNA reporter was selected for further application because of its relative greater degree of signal change and smaller standard error (Figure 2 H). With the completion of the surface packing optimization, we tested the storage stability of the optimized ssDNA electrode by storing at 4 °C in a humidified environment (Supporting Information, Figure S4). A stable SWV signal was retained for around 3 days, which is a sufficient turnaround time for a clinical point-of-care routine. If a longer storage stability is needed, a multi-component monolayer system can be applied as demonstrated previously to maintain a high sensitivity over months.[15] Moreover, a multi-component monolayer system (for example, ternary self-assembled monolayers) might also increase sensitivity through tuning the molecular packing on the surface.[16]

Another interesting finding regarding the cleavage accessibility is that Cas12a-crRNA-based trans-cleavage activity is also significantly concentration dependent, as is the case for the analogue Cas9.[17] Different concentrations of Cas12a-crRNA in response to a same target concentration were evaluated (Supporting Information, Figure S5). A high concentration level (greater than 100 nM) in a 30 μL sample solution significantly decreased the activity of the Cas12a endonuclease towards a nonspecific ssDNA reporter as the large size of Cas12a hinders its diffusion in the testing solution. Hence, a relative minor change in current outputs was observed when using a high concentration of Cas12a-crRNA. An optimized concentration for Cas12a-crRNA duplex trans-cleavage operation was identified to be 30 nM in a 30 μL solution.

E-CRISPR on Nucleic Acid Detection

Based on the optimized trans-cleavage conditions, we evaluated the E-CRISPR platform for the detection of HPV-16. A broad dynamic range (pM to μM) of more than three orders of magnitude was achieved with an IC_{50} value of 0.78 nM based on the samples prepared in the buffer solution (Figure 3 A). The dose-dependent response curve demonstrated an average standard error (SE) of 2.16% ($n = 3$), indicating a reliable reproducibility. An experimental limit of detection (LOD) of 50 pM was obtained. It is worth mentioning that this LOD surpasses the previously published LOD for non-enzymatically amplified nucleic-acid detection by over two orders of magnitude.[3b] Moreover, the detection performance in a complex matrix was also evaluated. An IC_{50} value in pooled human serum was 0.68 nM, which is comparable with the IC_{50} value (0.78 nM) in buffer solution, indicating a great potential of E-CRISPR in the direct analysis of biological samples. We also tested the effect of target length on the trans-cleavage signal by increasing the length of the HPV-16 targeting sequence from 40 mer to 100 mer in the L1-enconding region.[9] Compared with the detection performance of the 40 mer DNA target, the 100 mer DNA target presented a similar IC_{50} value (0.62 nM, Supporting Information, Figure S6), indicating that the length of the target would not interfere with the in vitro trans-cleavage activity of Cas12a.

To evaluate the generality of the detection strategy, we used the E-CRISPR system to detect ssDNA erthrovirus, Parvovirus B19 (PB-19), which is known to cause erythema infectiosum in children and pregnant women.[18] A dynamic detection range from pM to μM was achieved with an IC_{50} value of 0.60 nM (Supporting Information, Figure S7 A). The percentage of signal change was similar to that of detection performance by HPV-16, indicating the on-chip trans-cleavage activity would not be affected by different targets.

We further investigated the accuracy of the E-CRISPR platform. A scrambled sequence and PB-19 were applied to

 © 2019 Wiley-VCH Verlag GmbH & Co. KGaA, Weinheim

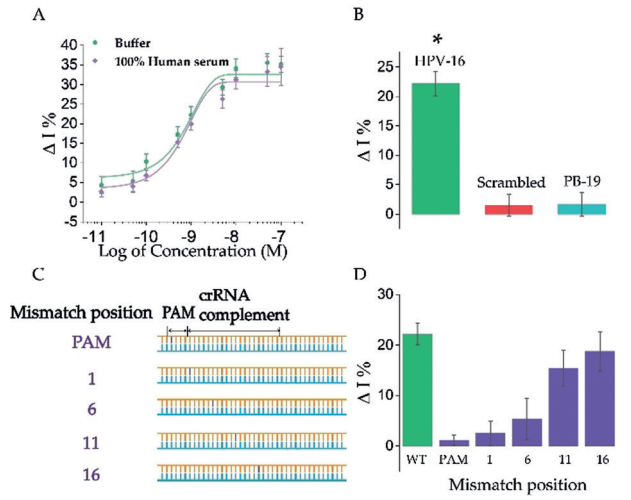


Figure 3. E-CRISPR analysis of HPV-16. A) Dose-response curve of the detection of HPV-16 in different matrixes (green line: 10 mM Tris buffer containing 50 mM NaCl and 15 mM $MgCl_2$; purple line: 100% human serum). B) Selectivity study through comparison of the signal changes based on non-target nucleic acids (500 nM) with that of 1 nM of HPV-16 ($n=3$, $^*P<0.01$, target signal vs. non-target signal). C) Target strands with mismatches at different positions, including PAM region and crRNA complement at different positions: 1, 6, 11, and 16. D) Evaluation of the influence of mismatches at different positions on the E-CRISPR signal. A target concentration of 1 nM was applied for all the targets (wild type (WT) and mismatched targets).

evaluate the selectivity for HPV-16 detection. 500 nM of scrambled sequence and PB-19 sequence demonstrated signal changes of less than 1.5% and 1.7%, respectively, which are lower than the standard error of the signal generated by 1 nM HPV-16 target, indicating a good selectivity of the Cas12a-crRNA duplex in differentiating HPV-16 from non-target (Figure 3B). A selectivity test was also performed for PB-19 detection using HPV-16 and scrambled sequence as interferences (Supporting Information, Figure S7B), demonstrating the reliable recognition activity of the CRISPR system.

Furthermore, as a biosensing platform, discrimination of mismatches in the nucleic acid base pairs is of importance for the potential application for the identification of disease related point mutations.[19] Thus, we next challenged the E-CRISPR with artificial mismatched nucleic acid targets (HPV-16). The recognition mechanism of CRISPR-Cas12a involves the identification of the PAM region on the target to unwind the DNA target by Cas protein and further hybridization between the crRNA and the target strand.[3a,14b] Therefore, we designed mismatches at different positions on the target (Figure 3C). E-CRISPR signal was obtained based on the detection of 1 nM of these artificial targets (Figure 3D). Compared with the wild type (WT) HPV-16 sequence, mutations in the PAM region and PAM-adjacent region (position 1) led to complete diminishment of the trans-cleavage signal. This phenomenon indicates the mandatory requirement of the PAM sequence for the Cas12a-crRNA duplex to recognize and cleave the target.[20] Moreover, mismatches in the complementary region of crRNA and the target resulted in decreased trans-cleavage activity, consistent with previous mismatch tolerance studies using Cas12a.[3a,21] The clear differentiable SWV signal between mismatches at different positions also suggests that the trans-cleavage activity of Cas12a might be utilized to identify the position of the mismatched base pairs as a biosensing strategy. Overall, E-CRISPR demonstrates a sensitive, generalized, and cost-effective platform for nucleic acid analysis.

Aptamer-Based E-CRISPR Cascade for Protein Detection

We next explored whether the E-CRISPR could be repurposed as a protein detection platform by utilizing the nucleic acid detection capability of E-CRISPR. For protein detection, an ssDNA aptamer was used as the recognition element for a protein of interest. An aptamer-based E-CRISPR cascade was designed for protein detection (Figure 4), which allows the direct analysis of complex sample without any time-consuming processing procedures. A fixed concentration of aptamer is firstly applied to treat the sample directly (Figure 4A). Cas12a-crRNA is designed to specifically recognize the aptamer. The E-CRISPR is then applied to determine the remaining concentration of aptamer in the sample (Figure 4B). In the presence of the protein target, less aptamer would be captured and transduced by E-CRISPR, leading to a high electrochemical signal of the MB from the ssDNA reporter. In the absence of the protein target, the electrochemical signal would be lower due to the activation of trans-cleavage activity by ssDNA target recognition (Figure 4C).

This designed E-CRISPR array was evaluated for the detection of transforming growth factor β1 (TGF-β1) protein, which is a secreted protein contributing to cell proliferation and differentiation,[22] and is also recognized as a biomarker for hepatocellular carcinoma.[23] The dose-dependent E-CRISPR for the detection of TGF-β1 aptamer was first evaluated using the previous established trans-cleavage conditions (Supporting Information, Figure S8). For proof-of-concept, a fixed concentration of aptamer was first applied to treat the sample with and without TGF-β1. E-CRISPR was then applied to analyze the samples with and without TGF-β1 demonstrating a clear signal difference (Supporting Information, Figure S9). In order to increase the detection resolution for nanomolar concentration range, a greater degree of current difference between 1 nM and 50 nM is necessary. Therefore, a longer trans-cleavage period was investigated to evaluate whether a higher current difference can be obtained as the trans-cleavage activity is a multiple-turnover reaction.[3a] Increasing trans-cleavage period indeed leads to a higher detection resolution (Supporting Information, Figure S8B), so a trans-cleavage period of 60 min was selected for protein detection. Therefore, this strategy might be applied to tune the dynamic range and detection limit of the E-CRISPR platform, enhancing the detection performance. An aptamer concentration of 50 nM was selected for protein sample treatment for 30 min. After the treatment, the sample was evaluated by E-CRISPR. A linear detection range was achieved covering three order of magnitudes with an LOD of 0.2 nM (Figure 4D). The detection specificity was investigated using conditioned cell medium from human mesen-

© 2019 Wiley-VCH Verlag GmbH & Co. KGaA, Weinheim

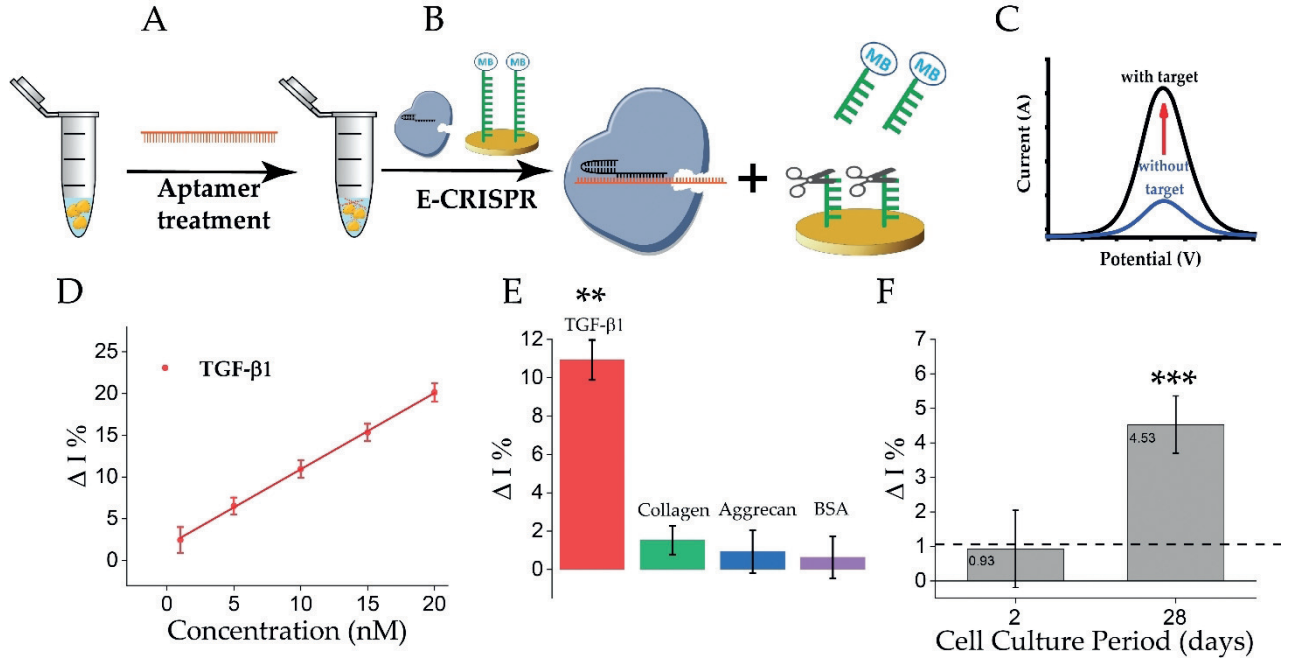


Figure 4. E-CRISPR cascade for protein detection. A) Sample containing protein target of interest is firstly treated by a fixed concentration of target-specific aptamer (ssDNA). B) A E-CRISPR system is specifically designed for the recognition of the aptamer. The remaining concentration of aptamer is analyzed by E-CRISPR. C) A representation of SWV results in the presence and absence of the target. D) Linear calibration curve of TGF-β1 detection with an equation of $Y = 0.91X + 1.79$ and R-square value of 0.99 ($n = 3$, SE = 1.54%). E) Selectivity study through comparison of the signal outputs in the presence of 10 nM non-target proteins with that obtained in the presence of 10 nM TGF-β1 ($n = 3$, $^{**}P < 0.01$ versus different interference substances). F) Concentration-dependent signals observed within conditioned cell medium harvested at two time-points during the chondrogenic differentiation program of human mesenchymal stem cells (hMSCs) medium containing TGF-β1. The samples were analyzed by three sets of individual experiments using three different sensors ($n = 3$, $^{***}P < 0.05$, Day 28 vs. Day 2). The horizontal black dashed line represents the average signal variation ($n = 3$) in the presence of conditioned cell medium only.

chymal stem cells (hMSCs) chonodrogenesis, which is a complex matrix, including collagen type II, aggrecan protein, and bovine serum albumin. The designed strategy resulted in a good selectivity for the target protein over non-specific molecules, indicating an excellent specificity of the applied aptamer in the system (Figure 4E). We further challenged the E-CRISPR platform with samples obtained during the chondrogenic differentiation of hMSCs, which were cultured in aggregates with complete chondrogenic differentiation medium for 4 weeks.[24] TGF-β1 was produced during the chondrogenic differentiation process.[25] A clear difference was identified between the conditioned medium obtained at day 2 and day 28 (Figure 4F). These results are in agreement with the transcriptome analyses of the same samples performed during chondrogenesis of hMSCs (Supporting Information, Figure S10), indicating a reliable performance of the designed E-CRISPR array for protein detection. The nucleic-acid-based receptor is a generalized recognition element for both protein and small molecule.[26] Hence, the designed E-CRISPR array can also be extended to a wide variety of analytes.

Conclusion

This study introduces a new strategy for the development of electrochemical biosensors by using electrochemistry to probe the CRISPR cleavage activity (E-CRISPR). Owing to the high specificity of target recognition, more than a gene editing tool, we utilized the CRISPR Type V system, Cas12a (cpf1), as an efficient biosensing system, which translates the target recognition activity into a detectable electrochemical signal through an interrogating electrode constructed with non-specific ssDNA. Various factors were investigated to produce a high sensitivity E-CRISPR-based detection platform with an optimized on-chip trans-cleavage activity. Moreover, our preliminary implementation illustrates that the E-CRIPSR system can be applied not only for nucleic acid sensing; with the addition of an aptamer-based sensing cascade, the E-CRISPR can also be utilized for protein detection, providing a generalizable, robust, and cost-effective detection system.

Acknowledgements

The authors acknowledge the staff of the Electronics Design Center for the experimental support and Xintong Cao for the artwork. We acknowledge the funding supports from National Institute of Health under the grant number, NIBIB:1-P41EB021911 and R01DK113185. We also acknowledge the funding supports from Wallace R. Persons Research Fund from Case Alumni Association.

 © 2019 Wiley-VCH Verlag GmbH & Co. KGaA, Weinheim

Conflict of interest

The authors declare no conflict of interest.

Stichwörter: Bioanalytische Chemie · Biosensoren · CRISPR Cas12a (cpf1) · Elektrochemie · Trans-Spaltung

Zitierweise: *Angew. Chem. Int. Ed.* **2019**, *58*, 17399 – 17405
Angew. Chem. **2019**, *131*, 17560 – 17566

[1] a) S. O. Kelley, C. A. Mirkin, D. R. Walt, R. F. Ismagilov, M. Toner, E. H. Sargent, *Nat. Nanotechnol.* **2014**, *9*, 969; b) Y. Yang, W. Gao, *Chem. Soc. Rev.* **2019**, *48*, 1465 – 1491; c) J. Kim, A. S. Campbell, B. E.-F. de Ávila, J. Wang, *Nat. Biotechnol.* **2019**, *37*, 389 – 406; d) Y. Dai, C. C. Liu, *Angew. Chem. Int. Ed.* **2019**, *58*, 12355 – 12368; *Angew. Chem.* **2019**, *131*, 12483 – 12496; e) Y. Wu, R. D. Tilley, J. J. Gooding, *J. Am. Chem. Soc.* **2019**, *141*, 1162 – 1170; f) A. L. Furst, M. B. Francis, *Chem. Rev.* **2019**, *119*, 700 – 726; g) T. J. Zwang, E. C. M. Tse, J. K. Barton, *ACS Chem. Biol.* **2018**, *13*, 1799 – 1809; h) A. A. Lubin, K. W. Plaxco, *Acc. Chem. Res.* **2010**, *43*, 496 – 505; i) F. Yang, Q. Li, L. Wang, G.-J. Zhang, C. Fan, *ACS Sens.* **2018**, *3*, 903 – 919.

[2] a) J. S. Gootenberg, O. O. Abudayyeh, J. W. Lee, P. Essletzbichler, A. J. Dy, J. Joung, V. Verdine, N. Donghia, N. M. Daringer, C. A. Freije, *Science* **2017**, *356*, 438 – 442; b) Y. Li, S. Li, J. Wang, G. Liu, *Trends Biotechnol.* **2019**, *37*, 730 – 743; c) K. Leung, Y. Krishnan, *ACS Cent. Sci.* **2019**, *5*, 1111 – 1113; d) L. Cong, F. A. Ran, D. Cox, S. Lin, R. Barretto, N. Habib, P. D. Hsu, X. Wu, W. Jiang, L. A. Marraffini, *Science* **2013**, *339*, 819 – 823; e) T. P. Huang, K. T. Zhao, S. M. Miller, N. M. Gaudelli, B. L. Oakes, C. Fellmann, D. F. Savage, D. R. Liu, *Nat. Biotechnol.* **2019**, *37*, 626 – 631; f) J. H. Hu, S. M. Miller, M. H. Geurts, W. Tang, L. Chen, N. Sun, C. M. Zeina, X. Gao, H. A. Rees, Z. Lin, D. R. Liu, *Nature* **2018**, *556*, 57; g) H. Yin, C.-Q. Song, S. Suresh, S.-Y. Kwan, Q. Wu, S. Walsh, J. Ding, R. L. Bogorad, L. J. Zhu, S. A. Wolfe, V. Koteliansky, W. Xue, R. Langer, D. G. Anderson, *Nat. Chem. Biol.* **2018**, *14*, 311.

[3] a) J. S. Chen, E. Ma, L. B. Harrington, M. Da Costa, X. Tian, J. M. Palefsky, J. A. Doudna, *Science* **2018**, *360*, 436 – 439; b) J. S. Gootenberg, O. O. Abudayyeh, M. J. Kellner, J. Joung, J. J. Collins, F. Zhang, *Science* **2018**, *360*, 439 – 444; c) S.-Y. Li, Q.-X. Cheng, J.-M. Wang, X.-Y. Li, Z.-L. Zhang, S. Gao, R.-B. Cao, G.-P. Zhao, J. Wang, *Cell Discovery* **2018**, *4*, 20; d) S.-Y. Li, Q.-X. Cheng, J.-K. Liu, X.-Q. Nie, G.-P. Zhao, J. Wang, *Cell Res.* **2018**, *28*, 491.

[4] a) Y. Dai, C. Wang, L.-Y. Chiu, K. Abbasi, B. S. Tolbert, G. Sauvé, Y. Yen, C.-C. Liu, *Biosens. Bioelectron.* **2018**, *117*, 60 – 67; b) Y. Dai, K. Abbasi, S. Bandyopadhyay, C. C. Liu, *ACS Sens.* **2019**, *4*, 1980 – 1985.

[5] a) J. S. Chen, J. A. Doudna, *Nat. Rev. Chem.* **2017**, *1*, 0078; b) K. Murugan, K. Babu, R. Sundaresan, R. Rajan, D. G. Sashital, *Mol. Cell* **2017**, *68*, 15 – 25.

[6] R. Sundaresan, H. P. Parameshwaran, S. Yogesha, M. W. Keilbarth, R. Rajan, *Cell Rep.* **2017**, *21*, 3728 – 3739.

[7] E. O'Brien, M. E. Holt, M. K. Thompson, L. E. Salay, A. C. Ehlinger, W. J. Chazin, J. K. Barton, *Science* **2017**, *355*, eaag1789.

[8] L. Mirabello, M. Yeager, K. Yu, G. M. Clifford, Y. Xiao, B. Zhu, M. Cullen, J. F. Boland, N. Wentzensen, C. W. Nelson, T. Raine-Bennett, Z. Chen, S. Bass, L. Song, Q. Yang, M. Steinberg, L. Burdett, M. Dean, D. Roberson, J. Mitchell, T. Lorey, S. Franceschi, P. E. Castle, J. Walker, R. Zuna, A. R. Kreimer, D. C. Beachler, A. Hildesheim, P. Gonzalez, C. Porras, R. D. Burk, M. Schiffman, *Cell* **2017**, *170*, 1164 – 1174.e1166.

[9] K. Seedorf, G. Krämmer, M. Dürst, S. Suhai, W. G. Röwekamp, *Virology* **1985**, *145*, 181 – 185.

[10] G. Maule, A. Casini, C. Montagna, A. S. Ramalho, K. De Boeck, Z. Debyser, M. S. Carlon, G. Petris, A. Cereseto, *Nat. Commun.* **2019**, *10*, 1 – 11.

[11] a) Y. Li, Q. Zheng, C. Bao, S. Li, W. Guo, J. Zhao, D. Chen, J. Gu, X. He, S. Huang, *Cell Res.* **2015**, *25*, 981; b) J. Tabernero, H.-J. Lenz, S. Siena, A. Sobrero, A. Falcone, M. Ychou, Y. Humblet, O. Bouché, L. Mineur, C. Barone, *Lancet Oncol.* **2015**, *16*, 937 – 948.

[12] M. Breinig, A. Y. Schweitzer, A. M. Herianto, S. Revia, L. Schaefer, L. Wendler, A. C. Galvez, D. F. Tschaharganeh, *Nat. Methods* **2019**, *16*, 51.

[13] B. Zetsche, J. S. Gootenberg, O. O. Abudayyeh, I. M. Slaymaker, K. S. Makarova, P. Essletzbichler, S. E. Volz, J. Joung, J. van der Oost, A. Regev, E. V. Koonin, F. Zhang, *Cell* **2015**, *163*, 759 – 771.

[14] a) W. Yang, *Nat. Struct. Mol. Biol.* **2008**, *15*, 1228; b) D. C. Swarts, J. van der Oost, M. Jinek, *Mol. Cell* **2017**, *66*, 221 – 233.e224.

[15] F. Kuralay, S. Campuzano, J. Wang, *Talanta* **2012**, *99*, 155 – 160.

[16] a) J. Wu, S. Campuzano, C. Halford, D. A. Haake, J. Wang, *Anal. Chem.* **2010**, *82*, 8830 – 8837; b) S. Campuzano, F. Kuralay, M. J. Lobo-Castañón, M. Bartošík, K. Vyavahare, E. Paleček, D. A. Haake, J. Wang, *Biosens. Bioelectron.* **2011**, *26*, 3577 – 3583; c) S. Campuzano, F. Kuralay, J. Wang, *Electroanalysis* **2012**, *24*, 483 – 493.

[17] B. Maji, C. L. Moore, B. Zetsche, S. E. Volz, F. Zhang, M. D. Shoulders, A. Choudhary, *Nat. Chem. Biol.* **2017**, *13*, 9.

[18] N. S. Young, K. E. Brown, *N. Engl. J. Med.* **2004**, *350*, 586 – 597.

[19] a) J. Wang, *Anal. Chim. Acta* **2002**, *469*, 63 – 71; b) H. Schwarzenbach, D. S. Hoon, K. Pantel, *Nat. Rev. Cancer* **2011**, *11*, 426.

[20] a) D. Kim, J. Kim, J. K. Hur, K. W. Been, S.-h. Yoon, J.-S. Kim, *Nat. Biotechnol.* **2016**, *34*, 863; b) L. Gao, D. B. T. Cox, W. X. Yan, J. C. Manteiga, M. W. Schneider, T. Yamano, H. Nishimasu, O. Nureki, N. Crosetto, F. Zhang, *Nat. Biotechnol.* **2017**, *35*, 789.

[21] H. K. Kim, M. Song, J. Lee, A. V. Menon, S. Jung, Y.-M. Kang, J. W. Choi, E. Woo, H. C. Koh, J.-W. Nam, H. Kim, *Nat. Methods* **2016**, *14*, 153.

[22] X. Xu, L. Zheng, Q. Yuan, G. Zhen, J. L. Crane, X. Zhou, X. Cao, *Bone Res.* **2018**, *6*, 2.

[23] a) M. Iwasaki, K. Nakata, H. Nakahara, T. Nakase, T. Kimura, K. Kimata, A. Caplan, K. Ono, *Endocrinology* **1993**, *132*, 1603 – 1608; b) C. Coulouarn, V. M. Factor, S. S. Thorgeirsson, *Hepatology* **2008**, *47*, 2059 – 2067.

[24] R. A. Somoza, D. Correa, I. Labat, H. Sternberg, M. E. Forrest, A. M. Khalil, M. D. West, P. Tesar, A. I. Caplan, *Tissue Eng. Part A* **2018**, *24*, 335 – 350.

[25] a) Z. Li, L. Kupcsik, S. J. Yao, M. Alini, M. J. Stoddart, *J. Cell. Mol. Med.* **2010**, *14*, 1338 – 1346; b) N. Shinojima, A. Hossain, T. Takezaki, J. Fueyo, J. Gumin, F. Gao, F. Nwajei, F. C. Marini, M. Andreeff, J.-I. Kuratsu, *Cancer Res.* **2013**, *73*, 2333 – 2344.

[26] N. Nakatsuka, K.-A. Yang, J. M. Abendroth, K. M. Cheung, X. Xu, H. Yang, C. Zhao, B. Zhu, Y. S. Rim, Y. Yang, P. S. Weiss, M. N. Stojanović, A. M. Andrews, *Science* **2018**, *362*, 319.

[27] D. P. Lennon, A. I. Caplan, *Exp. Hematol.* **2006**, *34*, 1604 – 1605.

Manuskript erhalten: 22. August 2019
Veränderte Fassung erhalten: 23. September 2019
Akzeptierte Fassung online: 30. September 2019
Endgültige Fassung online: 17. Oktober 2019

© 2019 Wiley-VCH Verlag GmbH & Co. KGaA, Weinheim